Scientific Reports

https://doi.org/10.1038/s41598-026-59994-7

Article in Press

Line waves at the interface of magneto–electric boundaries

Received: 11 May 2026

Accepted: 24 June 2026

Published online: 15 July 2026

Cite this article as: Ahmadi Z., Ahmadi H., Abdollahvand M. *et al.* Line waves at the interface of magneto–electric boundaries. *Sci Rep* (2026). https://doi.org/10.1038/s41598-026-59994-7

Zahra Ahmadi, Hadi Ahmadi, Mousa Abdollahvand, Hamed Saghaei, Sima Sobhi-Givi & Zahriladha Zakaria

Line Waves at the interface of Magneto-Electric Boundaries

Zahra Ahmadi[1], Hadi Ahmadi[2], Mousa Abdollahvband[3*], Hamed Saghaei[4], Sima Sobhi-Givi[3], and Zahriladha Zakaria[5]

[1]Department of Electrical Engineering, Tarbiat Modares University, Tehran, Iran

[2]Department of Electrical Engineering, Sharif University of Technology, Tehran, Iran

[3]Department of Electrical and Computer Engineering, University of Mohaghegh Ardabili, Ardabil, Iran.

[4]Department of Electrical Engineering, Shahrekord Branch, Islamic Azad University, Shahrekord, Iran

[5]Centre for Telecommunication Research & Innovation (CeTRI), Faculty of Electronic and Computer Technology and Engineering, Universiti Teknikal Malaysia Melaka (UTeM), Melaka, MALAYSIA.

***Corresponding author: Mousa Abdollahvand, Department of Electrical and Computer Engineering, University of Mohaghegh Ardabili, Ardabil, Iran (Email: m.abdollahvand@uma.ac.ir).**

Abstract

Line waves (LWs) are a unique class of electromagnetic modes confined to the interface between impedance surfaces, governed by electromagnetic duality. To date, most realizations of LWs have relied exclusively on electric impedance surfaces. In this work, we demonstrate that a planar interface between an electric impedance surface and a purely magnetic medium can support backscattering-immune LWs. The magnetic medium ($\varepsilon = 1, \mu \neq 1$) sustains TE-polarized surface magnon polaritons (SMPs), while the electric impedance surface supports TM-polarized surface waves. The coupling of these orthogonally polarized modes gives rise to a one dimensional, pseudospin filtered propagation channel. A comprehensive theoretical framework, supported by full-wave simulations, is developed to analyze dispersion characteristics, field confinement, and spin-momentum locking. The proposed structure enables ultra-confined wave guiding and offers a new platform for manipulating light matter interactions at terahertz frequencies. These findings open new avenues for magneto-electric waveguides and

pseudospin-controlled photonic devices.

1. Introduction

Spin waves are fundamental quasiparticles associated with the collective oscillation of magnetic moments in ordered media [1]. These waves enable the transport of spin information without the physical movement of charge carriers, thereby significantly reducing Joule heating losses compared to conventional electronic conduction [2]. In this context, spin waves are often described in terms of magnons, which represent quantized collective spin excitations within a lattice, analogous to phonons in crystal structures [2]. Owing to their wide operational frequency range, spanning from gigahertz to several hundred terahertz [3, 4], and spin waves have attracted considerable attention for next-generation information processing and wave based computing platforms.

Surface magnon polaritons (SMPs) arise from the strong coupling between electromagnetic waves and magnetic dipole oscillations at the interface of magnetic materials [5]. Similar to surface plasmon polaritons and phonon polaritons, SMPs exhibit hybrid light matter characteristics, enabling subwavelength field confinement and enhanced light matter interactions. These modes can be supported either in natural magnetic materials, such as antiferromagnetic crystals, or in artificially engineered metamaterials whose electromagnetic response is primarily governed by their structural design rather than intrinsic material properties [6]. The ability to manipulate SMPs at terahertz frequencies provides a powerful mechanism for controlling electromagnetic wave propagation in compact and integrated platforms.

In parallel, recent studies have introduced a novel class of electromagnetic modes known as line waves (LWs), which propagate along the one-dimensional interface between two impedance surfaces with complementary or dual boundary conditions [7–17]. Unlike conventional surface waves, which are confined to two dimensional interfaces, LWs are localized along infinitesimal lines where discontinuities in surface impedance occur [18].

These modes exhibit several remarkable properties, including strong field confinement, broadband behavior, robustness against structural perturbations, and polarization-dependent propagation characteristics, making them promising candidates for applications in sub-diffraction imaging, sensing, and integrated photonic circuits [19].

Despite the rapid progress in LW research, most reported implementations rely exclusively on electric impedance surfaces to support TM polarized surface waves. The role of magnetic media, particularly in enabling TE-polarized surface modes and their interaction with electric surfaces, has remained largely unexplored. In particular, the integration of surface magnon polaritons into LW platforms has not yet been investigated, leaving a significant gap in the development of magneto-electric waveguiding mechanisms.

In this work, we address this gap by demonstrating that a planar interface between an electric impedance surface and a purely magnetic medium can support a new class of line waves. In the proposed structure, the electric impedance surface sustains TM polarized surface waves, while the magnetic medium ($\varepsilon = 1$, $\mu \neq 1$) supports TE polarized surface magnon polaritons. The coupling of these orthogonally polarized modes gives rise to a one-dimensional propagation channel exhibiting pseudospin momentum locking and backscattering immune behavior. We further analyze the dispersion characteristics of SMPs in a finite thickness magnetic slab and investigate the formation and propagation of LWs at the magneto-electric interface. The proposed configuration enables pseudospin filtered waveguiding and provides a versatile platform for manipulating electromagnetic waves at terahertz frequencies.

2. Theoretical Model and Structure Design

Fig. 1 depicts a schematic configuration in which an inductive impedance surface is interfaced with a magnetic slab within a three-dimensional Cartesian coordinate system. The impedance surface is situated in free space on the x–y plane for $x \le 0$, while the magnetic medium occupies the region $x > 0$. The electric surface satisfies an isotropic impedance boundary condition [20]:

$$Z_s = \frac{E_t}{H_t} \tag{1}$$

where the subscript t denotes to the tangential components of the electromagnetic fields. According to [8], the surface impedance can be represented using a dimensionless parameter ζ, representing an inductive response (Z_s) as:

$$Z_s = j\frac{\eta_0}{\zeta},\ \text{if}\ x<0 \tag{2}$$

Here, ζ is a real, dimensionless parameter defined as $\zeta = |j\eta_0 / Z_s|$, and η_0 represents the intrinsic impedance of free space.

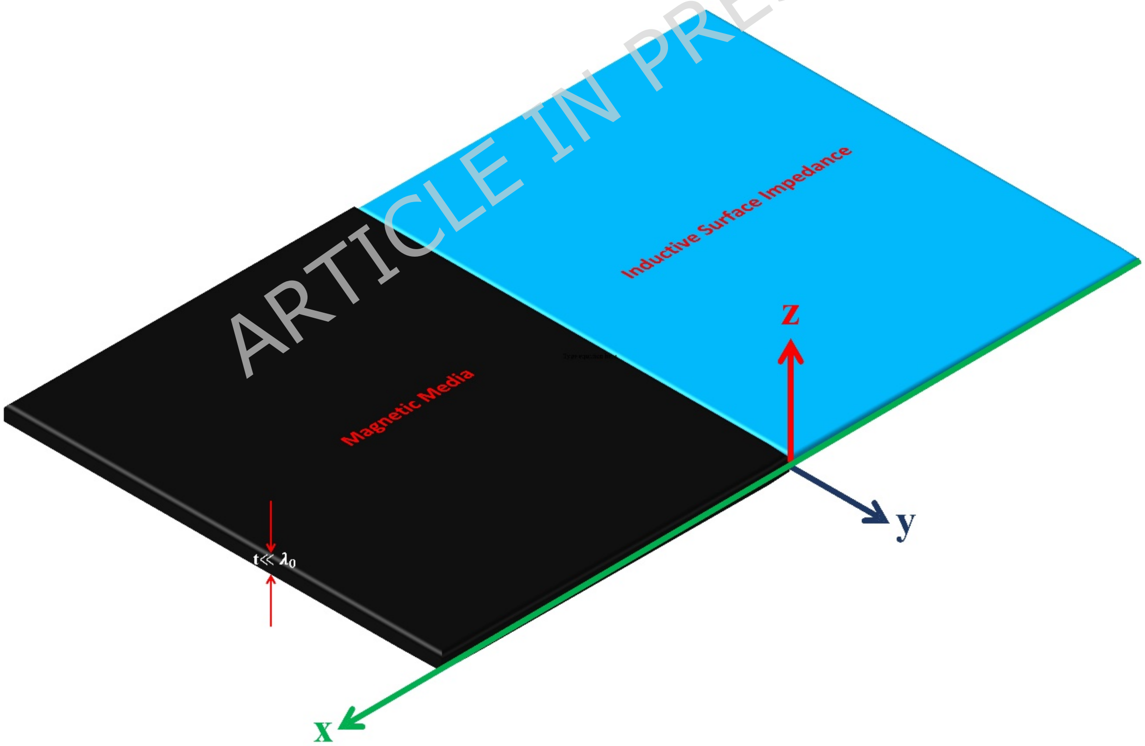

Fig. 1. A diagram illustrates the proposed setup where a magneto-electric junction enables a novel type of line wave.

The impedance surface supports the propagation of a TM-polarized surface wave when the surface reactance is inductive. Under this condition, the wave propagates along the *y*-direction without attenuation, while exhibiting exponential decay away from the surface in the transverse direction. The corresponding propagation constant is denoted by

$$\beta_{TM} = k_0\sqrt{1-\left(\frac{\eta_0}{Z_s}\right)^2} \tag{3}$$

where $k_0 = \frac{2\pi}{\lambda_0} = \omega\sqrt{\mu_0\varepsilon_0}$ is the free-space wavenumber (also called the propagation constant in vacuum).

Fig. 2 (a) illustrates the dispersion characteristics of the TM-polarized surface wave supported by the inductive impedance surface. As observed, increasing the parameter ζ leads to reduced field confinement near the surface. The confinement factor, defined as $\mathrm{Re}\{\beta/k_0\}$, ranges from 1.006 to 10 at a frequency of 6 THz for $1.3 < \zeta < 10$, indicating a gradual transition from weak to strong confinement regimes.

Analogous to surface plasmon polaritons, surface magnon polaritons are electromagnetic waves that propagate along the interface between a magnetic medium and a dielectric. These waves arise from the coupling between electromagnetic fields and spin-wave excitations in the magnetic material. Previous studies have extensively examined surface waves such as plasmons, phonons, and their hybrid forms. However, the role of purely magnetic materials in supporting TE-polarized surface magnon polaritons, particularly in the context of leaky-wave (LW) structures, remains largely unexplored. The electromagnetic properties of the magnetic medium are characterized by three parameters: relative permittivity $\varepsilon_r = 1$, relative permeability $\mu_r \geq 1$, and magnetic loss tangent $\tan(\delta_m)$ [20, 21]. In this work, we analyze TE-polarized surface wave propagation in a magnetic slab of finite thickness t=λ_0/200, as depicted in Fig. 2(b). The slab consists of a purely magnetic material with permittivity $\varepsilon = \varepsilon_0$ and permeability $\mu = \mu_r\mu_0$, while the surrounding regions (above and below) are free space. By enforcing the boundary conditions at the slab interfaces, the following eigenvalue equation governing the supported surface modes is obtained:

$$\left(\mu_r\mu_0\delta_0 - \mu_0\delta_1\right)^2 = \left(\mu_r\mu_0\delta_0 + \mu_0\delta_1\right)^2 \exp\left(-2\delta_1 t\right) \quad (4)$$

where the transverse decay constants are defined as $\delta_0 = \sqrt{\beta^2 - k_0^2}$, $\delta_1 = \sqrt{\beta^2 - \omega^2\varepsilon_0\mu_r\mu_0}$. The eigenvalue equation governing the TE-polarized surface modes (Eq. 4) is derived by enforcing the continuity of the tangential electric and magnetic field components at both interfaces of the finite-thickness magnetic slab. Fig. 2(b) illustrates the dispersion characteristics of the TE-polarized surface wave supported by the magnetic slab. The results indicate that the confinement factor, defined as $\mathrm{Re}\{\beta/k_0\}$, varies within the range $1.06 < \mathrm{Re}\{\beta/k_0\} < 4.1$ for $10.5 < \mu_r < 40$. This demonstrates that increasing the relative permeability enhances the surface wave confinement within the slab.

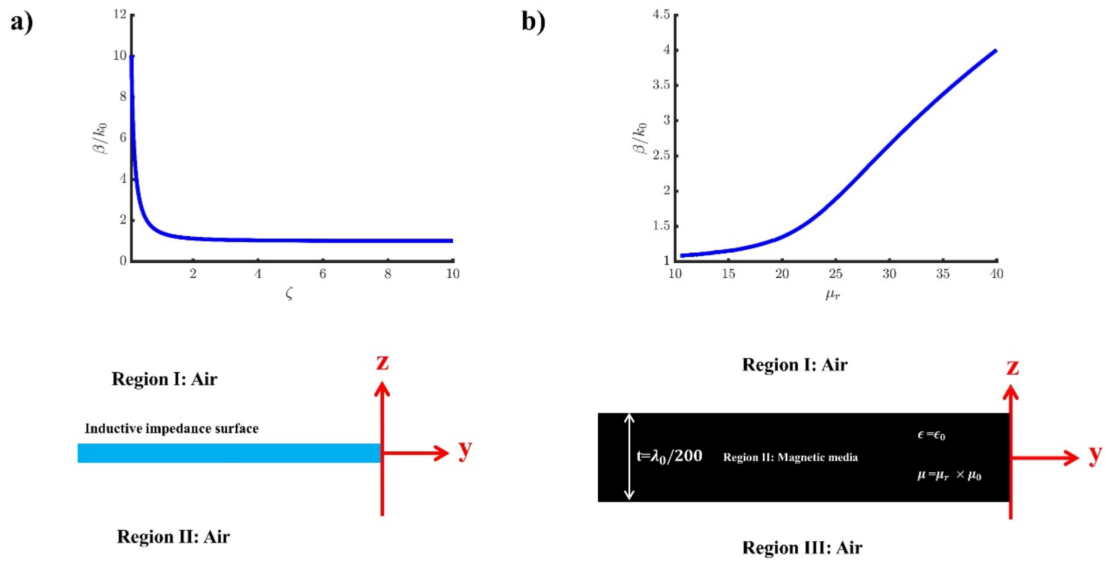

Fig. 2. Propagation constant of surface waves at a frequency of 6THz for (a) the electric impedance surface, and (b) the magnetic media.

Figure 3(a) presents the cross-sectional distribution of the electric field for the proposed line waveguide. The field is strongly confined along the interface, confirming the existence of a localized LW mode. Similar to LWs formed at the junction of complementary metasurfaces with identical unit-cell dimensions, the supported mode in this structure exhibits asymmetric field confinement on the two sides of the interface. This asymmetry originates from the dissimilar electromagnetic responses of the adjoining surfaces (TM-supporting impedance surface versus TE-supporting magnetic slab). As demonstrated in our previous work, such asymmetry can be mitigated by employing a bilayer configuration, which restores field balance across the interface. Figure 3(b) illustrates the corresponding vector-field distribution of the LW mode. The electric field is oriented tangentially along the TE-supporting surface, while it is normal (perpendicular) to the TM-supporting surface. This orthogonal alignment of the electric field components arises from the fundamentally different boundary conditions governing TE and TM surface waves. As a result, the superposition of these two surface-wave modes—with mutually perpendicular polarizations—produces a hybrid LW with an inclined (tilted) polarization state along the interface. In contrast, the magnetic field exhibits a complementary behavior: its orientation is orthogonal to that of the electric field, following Maxwell's equations. Consequently, the magnetic field vectors are reversed in orientation relative to the electric field distribution, maintaining the transverse electromagnetic nature of the guided LW mode.

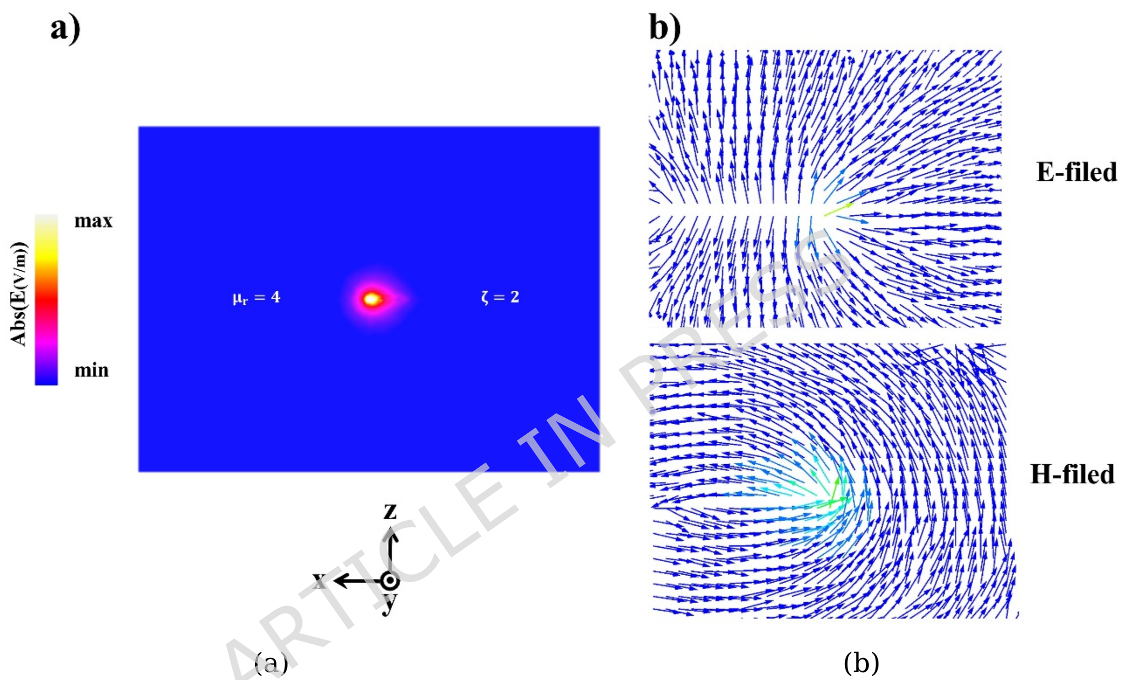

Fig. 3. (a) Field distribution of the one-dimensional wave over the cross-section of the waveguide. (b) Electric and magnetic fields vector distributions.

3. Pseudospin-filtering characteristics in LWs supported at the junction of magneto-electric media

Pseudospin-polarized waveguides capable of suppressing backscattering were first introduced by Chen et al. [22]. However, the realization of unidirectional waveguiding enabled by purely magnetic media remains largely unexplored. In this work, we show that the proposed magneto-electric line waves LWs inherently exhibit spin–momentum locking, a property commonly associated with evanescent waves. This means that the direction of propagation is intrinsically linked to the wave's polarization (pseudospin state). Moreover, these LWs demonstrate chiral coupling when excited by circularly polarized sources. As illustrated in Fig. 4, a combined electric and magnetic dipole—referred to as a spin source—can selectively launch waves along the magneto-electric interface. The propagation direction depends on the handedness of the source: out-of-phase dipoles excite the pseudospin-up state (j^+), leading to propagation in one direction, while in-phase dipoles excite the pseudospin-down state (j^-), resulting in propagation in the opposite direction. This selective excitation is a direct consequence of the spin-dependent coupling between the source and the guided mode. The underlying mechanism is rooted in the mirror (inversion) symmetry of the structure. Specifically, the inductive impedance surface and the magnetic slab satisfy the relations $e(-x)=a_1 m(x)$, $m(-x)=a_2 e(x)$, where a_1 and a_2 are real constants. These symmetry conditions arise from the mirror pairing of the two media across the *y–z* plane. As a result, the interface supports a unique spin-momentum-locked mode that is inherently robust against backscattering from certain classes of structural perturbations, provided the symmetry is preserved.

To verify that the proposed waveguide maintains this symmetry-protected behavior, a T-junction configuration is considered, as shown in Fig. 5. When the pseudospin-up state is excited at port 1, the wave couples only into ports 2 and 3, corresponding to forward-propagating modes. Importantly, the structure allows only the forward-propagating spin-up mode, while suppressing any backward or spin-flipped components. At port 4, the modified boundary conditions break the required symmetry for mode conversion, thereby preventing any transition from the pseudospin-up state to the pseudospin-down state. Consequently, the proposed waveguide operates as a spin-selective (spin-filtered) channel, where only one pseudospin state can propagate in a given direction. Under excitation of the pseudospin-up forward mode, the line wave propagates without reflection, as long as the mirror symmetry of the structure is maintained. Alternatively, this is proved in Figure 5(b) where transmission and reflection between ports 1 and 4 demonstrate spin filtering.

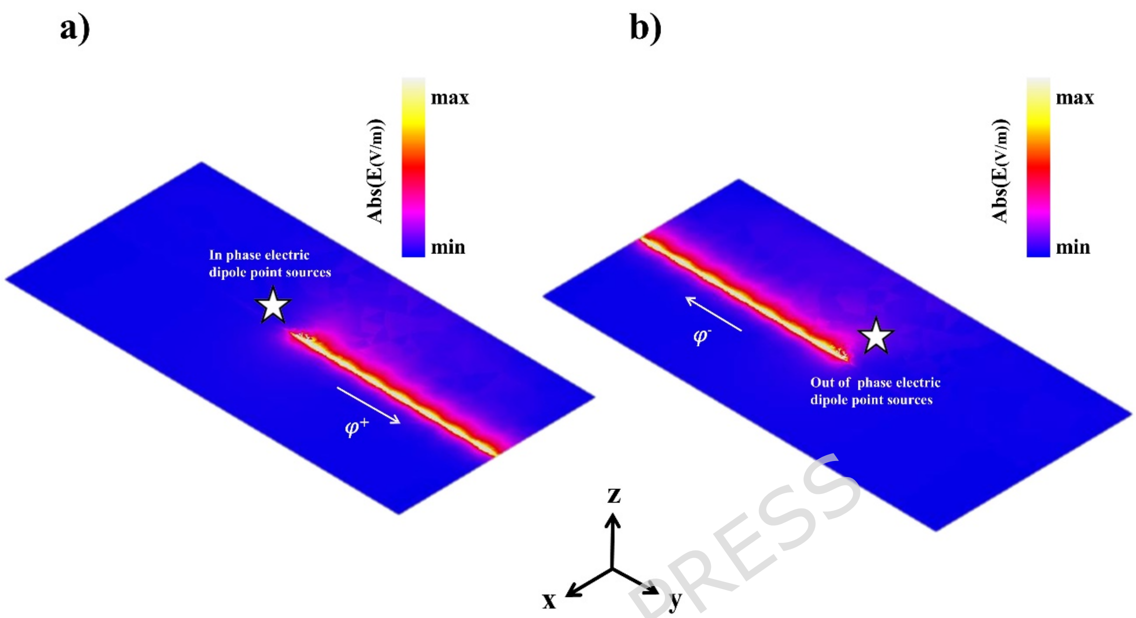

Fig. 4. Pseudospin states are excited by electric and magnetic Hertzian dipoles aligned along the z-axis, either (a) in phase or (b) out of phase.

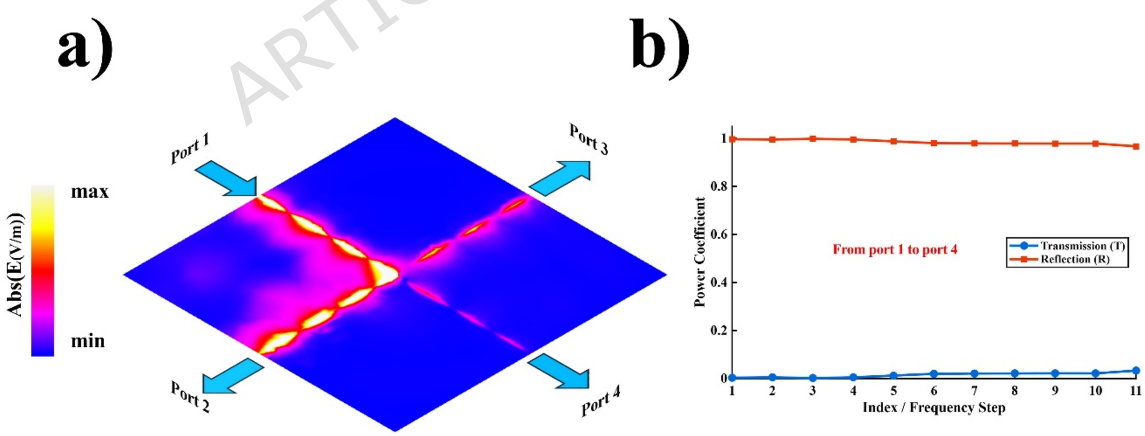

Fig. 5. (a)Proving spin-momentum locking feature in a magnetic waveguide. (b) Transmission and reflection from port 1 to port4.

4. Spin angular momentum of coupled line waves and eigen-mode analysis

Electromagnetic waves carry two fundamental forms of angular momentum: spin angular momentum (SAM) and orbital angular momentum (OAM). These intrinsic properties play a central role in light–matter interactions. SAM is associated with the polarization state of the wave and arises when the electric field vector traces a helical trajectory during propagation. In contrast, OAM is related to the spatial phase structure of the wave, particularly in fields with azimuthal phase variation. For example, vortex beams carry OAM proportional to their topological charge [24]. Different classes of electromagnetic waves exhibit distinct spin characteristics. Evanescent waves and tightly focused beams possess transverse spin angular momentum, oriented perpendicular to the direction of propagation. Conversely, circularly polarized plane waves in free space exhibit longitudinal spin angular momentum, aligned with the propagation direction. Unlike conventional waveguiding modes, the proposed LW exhibits field confinement with exponential decay in two transverse directions, resulting in six nonzero electromagnetic field components. While the LW shares certain features with both TE and TM modes, it supports a hybrid field configuration with a distinct spin orientation, which fundamentally differentiates it from conventional guided waves. The local spin density of the electromagnetic field, expressed in units of $\hbar$ per photon, is given by [23]:

$$S=\left(E\times E^{*}+H\times H^{*}\right)/W \tag{5}$$

$$W=\left|E\right|^{2}+\left|H\right|^{2} \tag{6}$$

where W denotes the local electromagnetic energy density. Based on the pseudospin-state formalism, the proposed waveguide supports hybrid modes whose spin characteristics are determined by the combined electric and magnetic field distributions, enabling spin-dependent propagation behavior.

Fig. 6(a) illustrates the proposed magnetic–electric–magnetic platform, which supports coupled line modes through the interaction of distinct surface-wave mechanisms. As shown in Fig. 6(b), the coupling between two line waves reduces by increasing the gap d between two channels. In addition, a co-propagating surface wave guided by the inductive impedance surface is incorporated. In general, intrinsic SAM of electromagnetic waves can be categorized into three types: longitudinal SAM, aligned with the direction of propagation; transverse SAM, oriented perpendicular to the propagation direction; and a non-orthogonal (hybrid) spin component associated with LWs [23]. Fig. 6(c) presents the spatial distribution of the spin angular momentum density for a surface wave propagating along the y-axis. The field exhibits exponential decay in the x-direction, confirming its evanescent nature. This evanescence introduces an imaginary longitudinal field component, which induces a rotation of the electromagnetic fields in the y–z plane. As a result, a purely transverse spin angular momentum is generated, dominated by the electric field contribution ($S \approx S_e$, with $S_m \approx 0$). Notably, this transverse spin is momentum-locked but independent of helicity, which is a characteristic feature of evanescent waves. Fig. 6(d) shows the spin angular momentum density for the coupled line modes at different values of z. For lower z, both transverse and LW-specific (hybrid) spin components coexist, indicating a mixed polarization state. As z increases, the spin becomes predominantly transverse, corresponding to stronger confinement and reduced hybridization. Therefore, tuning z provides an effective means to control the spin characteristics of the supported line waves.

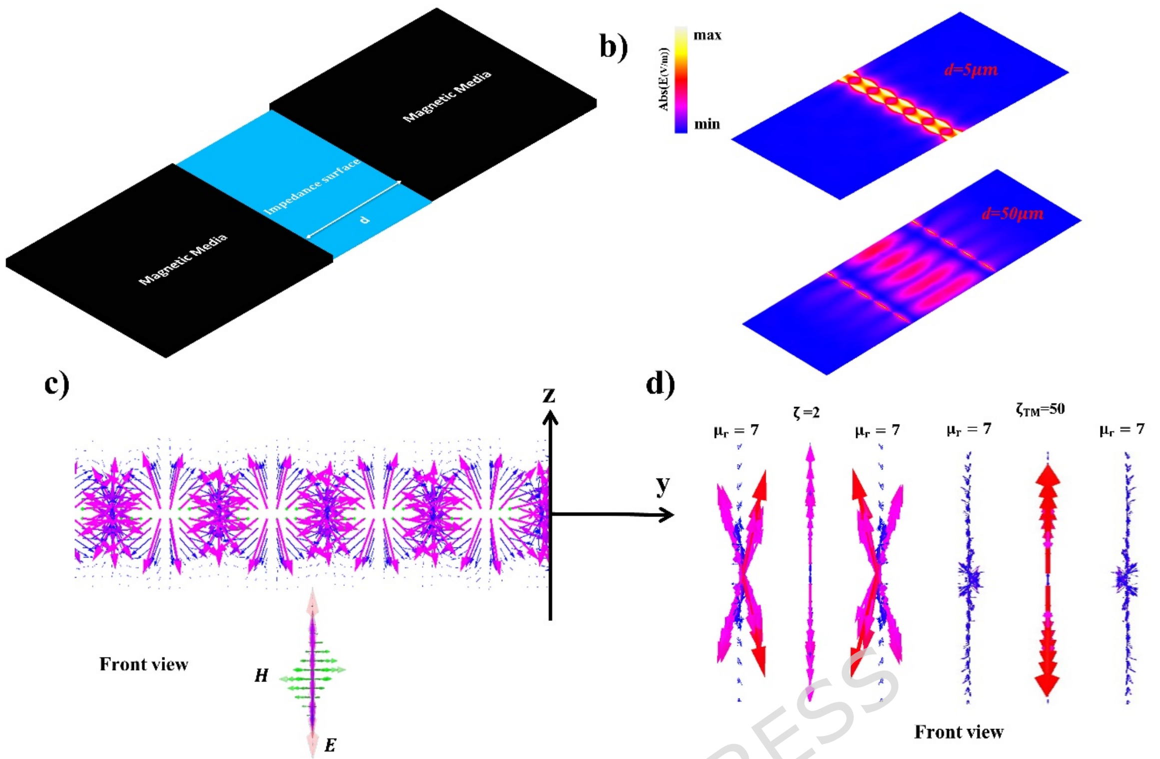

Fig. 6: (a) Configuration of a magnetic-electric-magnetic platform that supports coupled line modes, enabling effective interaction between different wave types. (b) Illustration of a co-propagating surface wave for different d values (c) Distribution of spin angular momentum density for a surface wave traveling along the y-axis, highlighting potential exponential decay in the x- direction. The wave exhibits evanescent properties, resulting in a rotation of electromagnetic fields within the y-z plane and producing purely transverse spin angular momentum from the electric field. (d) Spin angular momentum density for coupled line modes at varying ζ values. At lower ζ, both transverse and longitudinal wave (LW) spin angular momentum are present, whereas higher ζ values lead to predominantly transverse spin angular momentum.

Fig. 7 presents the propagation characteristics of the LW at a frequency of 6 THz for different values of ζ and μ_r. As shown in Fig. 7(a), when the relative permeability is fixed at $\mu_r=11$, the supported line mode within the range $0.3<\zeta<10$ exhibits a normalized propagation constant varying from $1.1 < \mathrm{Re}\{n_{eff}\} = \mathrm{Re}\left\{\frac{\beta}{k_0}\right\} < 9.04$. This indicates that increasing ζ significantly enhances the effective confinement of the guided mode. Furthermore, for a fixed $\zeta=2$, the variation of the magnetic response leads to a normalized propagation constant in the range $1.8 < \mathrm{Re}\{n_{eff}\} = \mathrm{Re}\left\{\frac{\beta}{k_0}\right\} < 3.56$ as μ_r increases from 11.15 to 38. This demonstrates that both the surface impedance parameter z and the relative permeability μ_r play crucial roles in controlling the dispersion and confinement of the supported line wave.

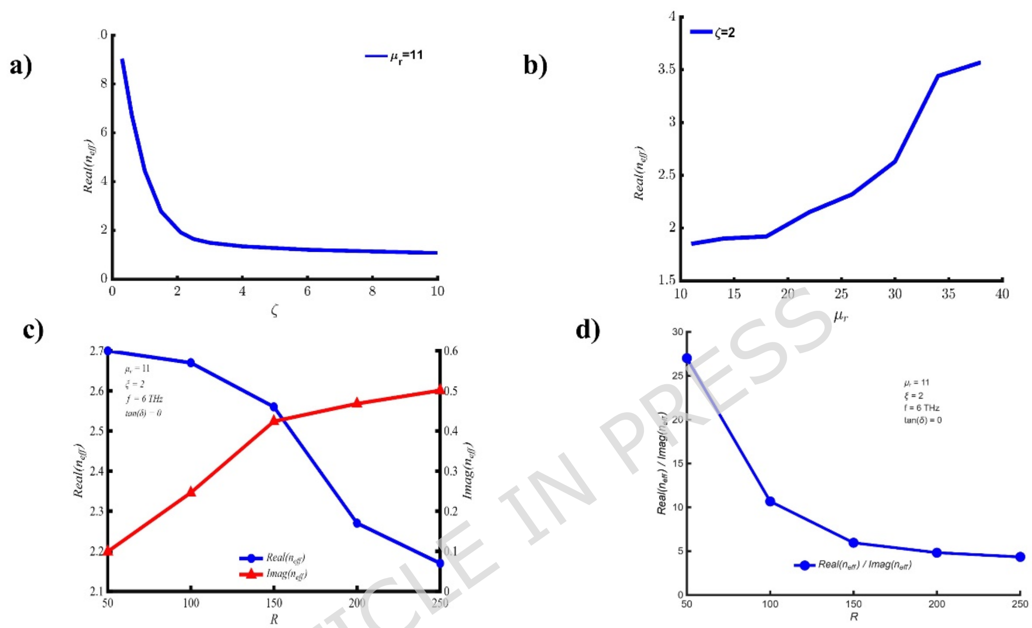

Fig. 7. Propagation characteristics of the LW at a frequency of 6 THz, (b) Representation of the normalized propagation constant for various values of μ and a fixed $\zeta = 2$. (c) Real and imaginary parts of the normalized propagation constant of the supported line wave as a function of R (d) Corresponding ratio of the real-to-imaginary parts of the effective refractive index, highlighting the modulation of the propagation length and modal confinement under varying structural parameters.

To further evaluate the impact of the structural parameter R on the propagation characteristics of the guided mode at 6 THz, Figs. 7(c) and 7(d) illustrate the complex effective refractive index and the corresponding propagation quality factor, respectively. As shown in Fig. 7(c), increasing R from 50 to 250 induces a pronounced decrease in the real part of the normalized propagation constant from approximately 2.7 to 2.17, indicating a transition toward a less tightly bound modal state. Concurrently, the imaginary part of n_{eff} exhibits a monotonic increase from 0.1 to 0.5, signifying elevated leakage or material attenuation as the field distribution shifts. This joint behavior is comprehensively captured in Fig. 2(d) by the sharp decline in the ratio of $Re\{n_{eff}\}/Imag\{n_{eff}\}$ which drops from over 25 to below 5, demonstrating that smaller values of R are critical for achieving highly confined, low-loss line-wave propagation with extended decay lengths along the magneto-electric interface.

It is worth noting that the asymmetric field distributions observed on the two sides of the magneto-electric interface may also be interpreted from a planar leaky-wave perspective. The guided line wave originates from the hybridization of TM-polarized and TE-polarized surface modes supported by the impedance surface and magnetic medium, respectively. Because these constituent surface waves possess different propagation constants, confinement factors, and attenuation characteristics, the coupled mode can excite slower surface-wave components with unequal leakage capabilities on the two sides of the interface. As a result, an asymmetric spatial field distribution naturally emerges. Similar planar-wave leakage and radiation mechanisms have recently been reported in metasurface platforms supporting analog flatland Cherenkov radiation, where guided surface modes continuously transfer energy into slower surface waves due to phase-matching conditions. Although the present work focuses on the formation and pseudospin properties of magneto-electric line waves, a detailed analysis of the associated surface-wave leakage, radiation mechanisms, and possible flatland Cherenkov-like phenomena represents an interesting avenue for future investigation [24].

5. Numerical Analysis and Practical Aspects

Full-wave electromagnetic (EM) simulations were performed using ANSYS HFSS, a commercially available software based on the finite element method. A Driven-mode setup was employed to investigate different configurations, which were excited by a source. For our calculations, a 3D parallelepiped computational domain with a height of λ0/2 along the z-axis was used, and two Wave Ports were positioned at the input and output of the waveguide to gather transmission data. HFSS Wave Ports require a uniform cross-sectional length at their connection points. The simulation begins with HFSS calculating a 2D solution for the wave port, which is then applied as the source for the 3D model. The process starts by solving the 2D fields on the port surface. The Eigenmode setup was employed to study dispersion relations, where the structure under investigation was modeled as two adjacent semi-infinite boundaries.

The proposed magneto-electric LW waveguide can be realized by combining grid-based electric metasurfaces with artificial magnetic metamaterials. On the electric side, the inductive impedance surface can be implemented using periodic metallic grids, where the effective surface impedance is engineered through appropriate unit-cell design. This enables the support of TM-polarized surface waves. On the magnetic side, metamaterials with approximately unity permittivity and enhanced permeability can be used to sustain TE-polarized surface magnon–polaritons. Such magnetic responses can be achieved using subwavelength resonant inclusions, and the overall structure is compatible with standard planar and multilayer fabrication techniques in the microwave and terahertz regimes. Due to the inherently resonant nature of magnetic metamaterials, the operational bandwidth of the proposed LW waveguide may be limited. However, this narrowband behavior is beneficial, as it promotes strong mode selectivity and enhanced field confinement at the magneto-electric interface.

Despite its limited bandwidth, the proposed LW waveguide offers several important advantages. The strong field localization along the line interface makes it highly suitable for sensing and detection applications, where small environmental perturbations can significantly modify the LW dispersion. Moreover, the inherent pseudospin–momentum locking enables backscattering-immune, spin-selective signal routing, which is particularly attractive for compact photonic, magnonic, and spintronic integrated systems. In addition, the structure can support applications such as narrowband filtering, chiral excitation, and reconfigurable waveguiding, especially when integrated with tunable magnetic or metamaterial platforms. Overall, the proposed approach provides a versatile framework for realizing highly confined, spin-controlled, and frequency-selective wave propagation

6. Conclusion

In conclusion, this study introduces a novel approach to implementing line-wave (LW) waveguides through a distinctive physical design. We uniquely examine pseudospin-momentum locking in magnetic waves, revealing the ability to control and transform the spin angular momentum of line waves. By investigating coupled line waves, we demonstrate how this control enables the conversion between linear and angular spin momentum states, expanding the functional versatility of LW-based systems. These findings offer significant implications for spintronic applications and contribute to the development of reconfigurable, polarization-controlled circuits. Additionally, our results pave the way for further exploration in manipulating spin-momentum interactions within similar waveguide systems, potentially enhancing future device performance across various frequency regimes and 2D materials. The proposed magneto-electric line-wave platform may exhibit scale-invariant waveguiding, where appropriate tuning of the magnetic permeability and impedance parameter preserves the normalized field distribution under geometric scaling. This would make the modal behavior depend primarily on dimensionless parameters rather than absolute size. Combined with spin-momentum locking, the structure could also support scale-invariant pseudospin-guided transport, offering an interesting direction for future research [25].

CRediT authorship contribution statement

Zahra Ahmadi: Writing – original draft, Methodology, Formal analysis, Conceptualization, Software, Investigation.

Hadi Ahmadi: Writing – review & editing, Validation, Formal analysis, Supervision.

Mousa Abdollahvand: Conceptualization, Methodology, Software, Investigation.

Hamed Saghaei: Validation, Writing – review & editing.

Sima Sobhi-Givi: Supervision, Writing – review & editing, Conceptualization.

Zahriladha Zakaria: Validation, Writing – review & editing, Conceptualization.

Declaration of competing interest

The authors declare the following financial interests/personal relationships which may be considered as potential competing interests: Mousa Abdollahvand reports a relationship with the University of Mohaghegh Ardabili, Department of Electrical Engineering, that includes academic affiliation. The authors declare that there are no conflicts of interest related to this submission. The remaining authors declare that they have no known competing financial interests or personal relationships that could have appeared to influence the work reported in this paper.

Data Availability

The datasets used and/or analyzed during the current study are available from the corresponding author upon reasonable request.

Funding

The authors received no specific funding for this work.

References

[1] G. Gurevich and G. A. Melkov, *Magnetization oscillations and waves* (CRC press, 2020).

[2] A. I. Akhiezer, V. G. Bar'yakhtar, and M. I. Kaganov, "Spin waves in ferromagnets and antiferromagnets. i," Uspekhi Fizicheskih Nauk **71**, 533–579 (1960).

[3] J. Van Kranendonk and J. Van Vleck, "Spin waves," Rev. Mod. Phys. **30**, 1 (1958).

[4] D. D. Stancil and A. Prabhakar, *Spin waves*, vol. 5 (Springer, 2009).

[5] J. Matsuura, M. Fukui, and O. Tada, "Atr mode of surface magnon polaritons on yig," Solid State Commun.**45**, 157–160 (1983).

[6] R. Macêdo and R. E. Camley, "Engineering terahertz surface magnon-polaritons in hyperbolic antiferromagnets," Phys. Rev. B **99**, 014437 (2019).

[7] S. Horsley and I. R. Hooper, "One dimensional electromagnetic waves on flat surfaces," J. Phys. D: Appl. Phys. **47**, 435103 (2014).

[8] D. J. Bisharat and D. F. Sievenpiper, "Guiding waves along an infinitesimal line between impedance surfaces," Phys. review letters **119**, 106802 (2017).

[9] D. J. Bisharat and D. F. Sievenpiper, "Electromagnetic-dual metasurfaces for topological states along a 1d

interface," Laser & Photonics Rev. **13**, 1900126 (2019).

[10] X. Kong, D. J. Bisharat, G. Xiao, and D. F. Sievenpiper, "Analytic theory of an edge mode between impedance surfaces," Phys. Rev. A **99**, 033842 (2019).

[11] Z. Xu, X. Yin, and D. F. Sievenpiper, "Adiabatic mode-matching techniques for coupling between conventional microwave transmission lines and one-dimensional impedance-interface waveguides," Phys. Rev. Appl. **11**, 044071 (2019).

[12] S. Singh, *Photonic Topological Insulators and their applications as Waveguides and Antennas* (University of California, San Diego, 2021).

[13] R. J. Davis, D. J. Bisharat, and D. F. Sievenpiper, "Classical-to-topological transmission line couplers," Appl. Phys. Lett. **118** (2021).

[14] Z. Xu, J. Chang, J. Tong, *et al.*, "Near-field chiral excitation of universal spin-momentum locking transport of edge waves in microwave metamaterials," Adv. Photonics **4**, 046004 (2022).

[15] M. Moccia, G. Castaldi, F. Monticone, and V. Galdi, "Exceptional points in flat optics: A non-hermitian line-wave scenario," Phys. Rev. Appl. **15**, 064067 (2021).

[16] Z. Xu, J. Chang, S. Fang, *et al.*, "Line waves existing at junctions of dual-impedance metasurfaces," ACS Photonics **8**, 2285–2293 (2021).

[17] M. Moccia, G. Castaldi, A. Alù, and V. Galdi, "Ghost line waves," ACS Photonics **10**, 1866–1872 (2023).

[18] A. Di Paola, M. Moccia, G. Castaldi, and V. Galdi, "Coupled line waves in parallel-plate metasurface waveguides," MRS Commun. **14**, 1255–1261 (2024).

[19] M. Moccia, G. Castaldi, A. Alu, and V. Galdi, "Line waves in non-hermitian metasurfaces," ACS Photonics **7**, 2064–2072 (2020).

[20] M. Hotta, M. Hano, and I. Awai, "Surface waves along a boundary of single negative material," IEICE transactions on electronics **88**, 275–278 (2005).

[21] R. Alexander and R. Bell, "Surface electromagnetic waves on magnetic media," Opt. Commun. **10**, 59–62 (1974).

[22] W.-J. Chen, Z.-Q. Zhang, J.-W. Dong, and C. Chan, "Symmetry-protected transport in a pseudospin-polarized waveguide," Nat. communications **6**, 8183 (2015).

[23] D. J. Bisharat and D. F. Sievenpiper, "Manipulating line waves in flat graphene for agile terahertz applications," Nanophotonics **7**, 893–903 (2018).

[24] Xu Z, Bao S, Liu J, Chang J, Kong X, Galdi V, Cui TJ. Observation of analog flatland Cherenkov radiations on metasurfaces. Laser & Photonics Reviews. 2024 Feb;18(2):2300763.

[25] Xu Z, Bao S, Moccia M, Castaldi G, Cui TJ, Galdi V. Scale-Invariant Waveguiding in Flatland. InExploration 2026 (p. 70108).